Journal of Convex Analysis
Volume 17 (2010), No. 3&4, 861–883

A New Relaxation Method for a Discrete Image Restoration Problem

M. Bergounioux
Université d'Orléans, UFR Sciences, Math., Labo. MAPMO, UMR 6628, Route de Chartres, BP 6759, 45067 Orléans cedex 2, France
maitine.bergounioux@univ-orleans.fr

M. Haddou
Université d'Orléans, UFR Sciences, Math., Labo. MAPMO, UMR 6628, Route de Chartres, BP 6759, 45067 Orléans cedex 2, France
mounir.haddou@univ-orleans.fr

Dedicated to Hedy Attouch on the occasion of his 60th birthday.

Received: December 09, 2008
Revised manuscript received: July 9, 2009

The method we present in this paper has been motivated by a restoration problem in a tomography context. We are interested in blurred and noised binary images restoration. We consider the discrete version of a minimization problem settled in the space of bounded variation functions. We give a general abstract formulation of the (discrete) optimization problem with binary constraints and provide approximate and penalized formulations. Convergence results are given and we present numerical tests.

Keywords: Tomography, optimization, penalization

1. Introduction

The method we present in this paper has been motivated by a restoration problem in a tomography context. The physical experiment as well as the modelling process have been precisely described in [1, 2]. We are interested here in a very specific application of tomographic reconstruction in order to study the behavior of a material under shock. During the deformation of the object, we obtain an X-ray radiography by high speed image capture. The research parameters maintain that the object is radially symmetric, so that one radiograph is enough to reconstruct the 3D object.

Physicists are looking for the shape of the interior at some fixed interest time. At the established time, the interior may be composed of several holes which also may be very irregular. We deal here with a synthetic object that contains all the standard difficulties that may appear (see Fig. 1.1). These difficulties are characterized by:

- Several disconnected holes.
- A small hole located on the symmetry axis (which is the area where the details are difficult to recover).

ISSN 0944-6532 / $ 2.50

- Smaller and smaller details on the boundary of the top hole in order to determine a lower bound for details detection.

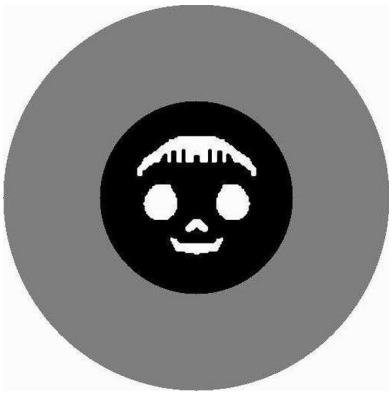

(a) Slice of a binary axially symmetric object by a plane containing the symmetry axis.

(b) Zoom on the interior of the object of Figure 1.1(a); the homogeneous material is drawn in black and the holes in white.

Figure 1.1: Working example

Our framework is completely different from the usual tomographic point of view and the usual techniques (such as filtered back-projection) are not appropriate to our case.

Let us make explicit the projection operator involved in the tomography process. This operator, denoted by $\mathcal{H}_o$, is given, for every function $f \in L^\infty(\mathbb{R}_+ \times \mathbb{R})$ with compact support, by

$$\forall (u,v) \in \mathbb{R} \times \mathbb{R} \quad \mathcal{H}_o f(u,v) = 2 \int_{|u|}^{+\infty} f(r,v) \frac{r}{\sqrt{r^2 - u^2}} dr. \tag{1}$$

For more details one can refer to [1, 2]. Similarly the adjoint operator $\mathcal{H}_o^*$ of $\mathcal{H}_o$ is

$$\forall (r,z) \in \mathbb{R} \times \mathbb{R}, \quad \mathcal{H}_o^* g(r,z) = 2 \int_0^{|r|} g(u,z) \frac{|r|}{\sqrt{r^2 - u^2}} du. \tag{2}$$

The symmetry of the object characterizes operator $\mathcal{H}_o$ as the Radon Transform of the object and so is invertible. However, the operator $\mathcal{H}_o^{-1}$ is not continuous with respect to the suitable topologies. Consequently, a small variation on the measure g leads to significant errors in the reconstruction. As radiographs are strongly perturbed, applying $\mathcal{H}_o^{-1}$ to data leads to a poor reconstruction. Due to the experimental setup there are two main perturbations:

- A blur, due to the detector response and the X-ray source spot size. We denote by $\mathcal{B}$ the effect of blurs and consider the simplified case where $\mathcal{B}$ is supposed to be linear.
- A noise which is supposed for simplicity to be an additive Gaussian white noise of mean 0, denoted by τ.

Consequently, the observed object u_d will be $u_d = \mathcal{B}(\mathcal{H}_o u) + \tau$. The comparison between the theoretical projection $\mathcal{H}_o u$ and the perturbed one is shown in Fig. 1.2 (b)–(c). The reconstruction using the inverse operator $\mathcal{H}_o^{-1}$ applied to u_d is given by Fig. 1.2 (d).

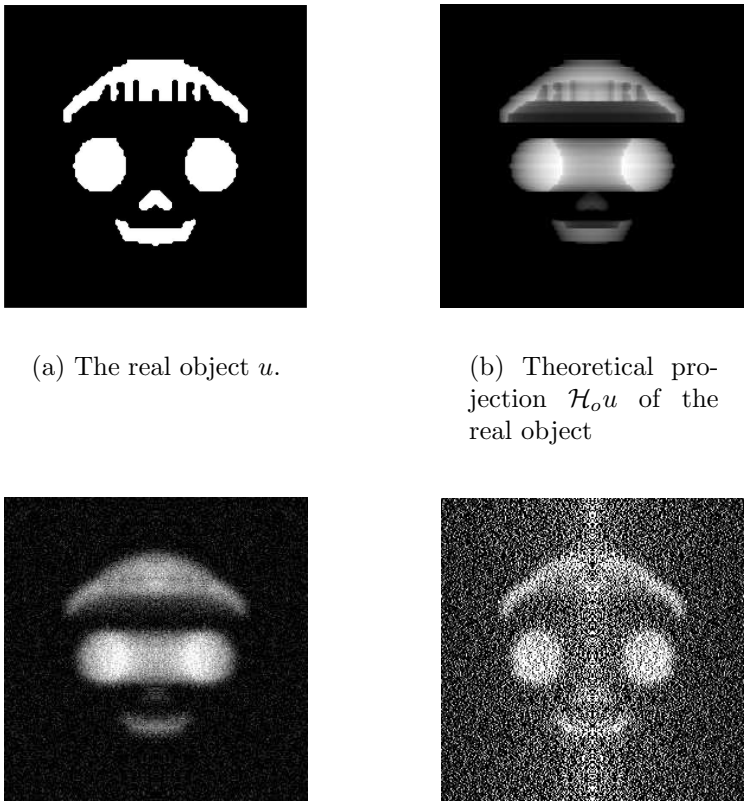

(a) The real object u.

(b) Theoretical projection $\mathcal{H}_o u$ of the real object

(c) Real projection $u_d = \mathcal{B}\mathcal{H}_o u + \tau$ of the same object with realistic noise and blur.

(d) Reconstruction $\mathcal{H}_o^{-1} u_d$ computed with $\mathcal{H}_o^{-1}$ applied to the real projection.

Figure 1.2: Comparison of u, $\mathcal{H}_o u$, $u_d = \mathcal{B}\mathcal{H}_o u + \tau$, $\mathcal{H}_o^{-1} u_d$.

It is clear from Fig. 1.2 (d) that the use of the inverse operator is not suitable. In the following examples we will call *experimental data* the image which corresponds to the blurred projection of a fictive object of density 0 with some holes of known density $\lambda > 0$ (we set $\lambda = 1$ in the sequel). Consequently, the space of admissible objects will be the set of functions f that take values $\{0, 1\}$. Such functions are defined on $\mathbb{R}^2$, have compact support included in an open bounded subset of $\mathbb{R}^2$, for example Ω and belong to the bounded variation functions space

$$BV(\Omega) = \{u \in L^1(\Omega) \mid \varphi(u) < +\infty\}$$

where $\varphi(u)$ stands for the total variation of u (see [3] for example). Abraham and al. [2] have investigated a variational model that can be applied to our situation. Let

$u_d \in L^2(\Omega)$ be the projected image (observed data).

$$\begin{cases} \min F(u) := \dfrac{1}{2}\|\mathcal{H}u - u_d\|_2^2 + \alpha\varphi(u), \\ u \in BV(\Omega), \\ u(x) \in \{0,1\} \quad \text{a.e. on } \Omega, \end{cases} \tag{3}$$

where $\|\cdot\|_2$ stands for the $L^2(\Omega)$ norm, $\alpha > 0$ and $\mathcal{H}$ is a linear operator (projection operator $\mathcal{H}_o$ composed with a linear blur operator or not). It is known from [2] that the above minimization problem admits at least one solution.

To solve (3), many numerical experiments are proposed in the litterature. Usually, people use the back-filtered projection method (see Fig. 1.3 below). In this case, results are of bad quality, as explained in [2].

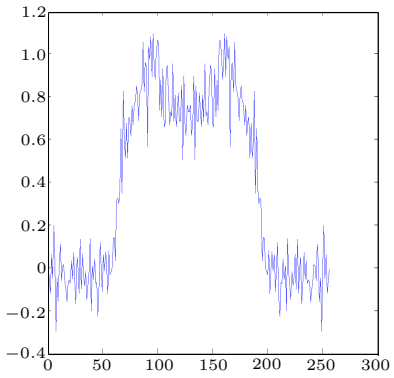

(a) Median line of the object ($i = 128$).

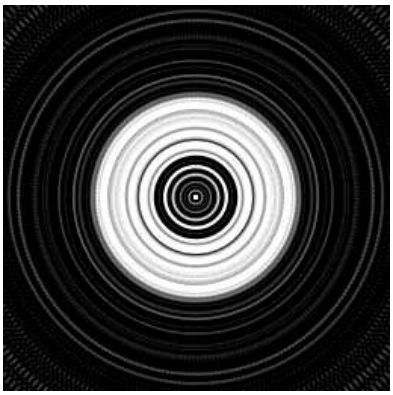

(b) Largest slice of the binary axially symmetric object by a plane orthogonal to the symmetry axis.

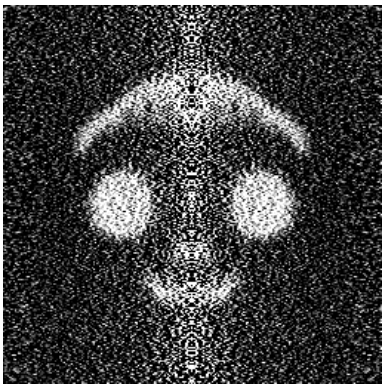

(c) Result using the cropped Ram-Lak filter.

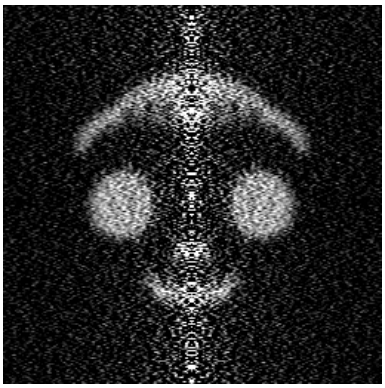

(d) Result using the Ram-Lak filter with a Hamming window.

Figure 1.3: Back-filtered projection results

In [1], the problem is studied via a shape optimization method. The object is viewed as a domain which optimal shape turns to be a solution. A derivative of the functional with respect to the domain is performed and a the level-set method [10] is used. With this method, an Hamilton-Jacobi equation involving non local terms has to be solved. The use of classical finite difference schemes gives acceptable results (see Fig. 1.4) but the method is time-consuming and highly unstable.

(a) Synthetic object (b) Computed solution

Figure 1.4: Level-set method results

An alternative method has been tested in [2]. The original problem (3) is penalized and its solution is computed with an *indirect method*: a first order optimality system is exhibited and a solution is computed. The results are good (see Fig. 1.5) but the process of parameters tuning is quite delicate. In addition, though the computation time is much shorter than the methods mentioned before, it remains quite long.

(a) Synthetic object (b) Computed solution

Figure 1.5: Penalization indirect method

In this paper we are mainly interested in the numerical computation of a solution and we consider a discrete version of problem (3) in order to use a *direct* method.

The next section is devoted to the discretization process of the problem described above. Here we give a general abstract formulation of the (discrete) optimization problem with binary constraints. In Sections 3 and 4 we give approximation (Section 3) and penalization (Section 4) formulations. The method is described and we provide convergence results. Section 5 is devoted to the numerical realization: here we detail the implementation and the results.

2. The finite dimensional problem

From now on because there is no ambiguity between the two, we will use the same notation for a function u living in a infinite dimensional framework as we do for the result of the discretization process which is a finite dimensional real vector.

2.1. The discrete problem

The discretization process is standard (see [4] for example). We give details in the last section devoted to numerical implementation. Once the discretization has been performed the original problem is approximated by the following discrete one

$$\begin{cases} \min \dfrac{1}{2}\|Hu - u_d\|_N^2 + \lambda\Phi(u), \\ u \in \mathbb{R}^N,\ u_i \in \{0,1\} \ \text{ for every } i = 1, \cdots, N. \end{cases} \tag{4}$$

Here

- u (resp. u_d) is a $\mathbb{R}^N$ vector representing the re-arranged $N_1 \times N_2$ image $(u_{i,j})_{1\leq i\leq N_1, 1\leq, j\leq N_2}$ with $N = N_1 N_2$,
- H is the real $N \times N$ matrix representing the blurred projection operator $\mathcal{BH}_o$
- $\Phi(u)$ is an approximation of the total variation. It is a convex, non differentiable function from $\mathbb{R}^N$ to $\mathbb{R}^+$. (Details are given in Section 5)
- $\|\cdot\|_N$ is the euclidian $\mathbb{R}^N$ norm and $(\cdot,\cdot)_N$ stands for the classical inner $\mathbb{R}^N$ product.

The difficulties that appeared in the infinite dimensional framework still remain that:

- the objective function is non differentiable because of Φ
- the *binarity* constraint $u \in \{0,1\}$ is difficult to resolve.

The first difficulty can be easily overcome using a smooth approximation of Φ. Indeed we have the generic result

Theorem 2.1. *Consider a function Ψ from $\mathbb{R}^N$ to $\mathbb{R}$, a nonempty finite subset K of $\mathbb{R}^N$ and any sequence of functions Ψ_ε such that*

$$\lim_{\varepsilon\to 0} \|\Psi_\varepsilon - \Psi\|_\infty = 0, \tag{5}$$

($\|\cdot\|_\infty$ is the $R^N - \ell^\infty$ norm). For ε small enough, we have

i) the optimal solution set $\mathcal{S}_\varepsilon$ of the optimization problem: $\min\{\Psi_\varepsilon(x) \mid x \in K\}$ *is a subset of the optimal solution set $\mathcal{S}$ of the optimization problem:* $\min\{\Psi(x) \mid x \in K\}$

ii) *If in addition, if*

$$\forall (x,y) \in K \times K \quad \Psi(x) = \Psi(y) \Rightarrow \Psi_\varepsilon(x) = \Psi_\varepsilon(y) \tag{6}$$

then $\mathcal{S}_\varepsilon = \mathcal{S}$.

Proof. *i)* Let v^* be the optimal value of the optimization problem (P) and define $\delta > 0$ by

$$\delta := \min_{x \in K \setminus \mathcal{S}} \psi(x) - v^*.$$

$\forall x \in \mathcal{S}$ and $\forall y \notin \mathcal{S}$ and ε small enough we have

$$\Psi_\varepsilon(x) \leq v^* + \frac{\delta}{2} \quad \text{and} \quad \Psi_\varepsilon(y) > v^* + \frac{\delta}{2}.$$

We can then conclude that $\mathcal{S}_\varepsilon \subset \mathcal{S}$, since outside of $\mathcal{S}$ we have $\Psi_\varepsilon > v^* + \frac{\delta}{2}$.

ii) It remains to prove $\mathcal{S} \subset \mathcal{S}_\varepsilon$. Let x be in $\mathcal{S}$. For any $\varepsilon > 0, \Psi(x) \leq \Psi(x_\varepsilon)$. For ε small enough $x_\varepsilon \in \mathcal{S}$ (with point i)). So $\Psi(x) \leq \Psi(x_\varepsilon) \leq \Psi(x)$. Assumption (6) gives $\Psi_\varepsilon(x) = \Psi_\varepsilon(x_\varepsilon)$. This means that $x \in \mathcal{S}_\varepsilon$. □

In our case the feasible domain

$$K := \mathbf{C} = \{u \in \mathbb{R}^N \mid u_i \in \{0,1\},\ i = 1, \cdots, N\},$$

is finite. Let Φ_ε be a smooth approximation of Φ satisfying assumptions (5) and (6). This leads to

$$\begin{cases} \min \dfrac{1}{2}\|Hu - u_d\|_N^2 + \lambda \Phi_\varepsilon(u), \\ u \in \mathbf{C}. \end{cases} \tag{7}$$

Problems (4) and (7) fit the assumptions of Theorem 2.1 with $\Psi(u) = \|Hu - u_d\|_N^2 + \lambda\Phi(u)$ and $\Psi_\varepsilon(u) = \|Hu - u_d\|_N^2 + \lambda\Phi_\varepsilon(u)$ so that we may conclude that for ε small enough problem (4) and (7) have the same solutions. In the sequel we need a $\mathcal{C}^2$ approximation Φ_ε of Φ to derive optimality conditions. A generic formulation of Φ is

$$\Phi(u) = \sum_{i=1}^{N} |(Du)_i|$$

where Du is a linear operator. We may choose for example

$$\Phi_\varepsilon(u) = \sum_{i=1}^{N} \sqrt{|(Du)_i|^2 + \varepsilon^2}$$

to approximate Φ. In this case (5) and (6) are satisfied and results (i, ii) of Theorem 2.1 hold.

2.2. An abstract formulation

From now on, we consider problem (4)

$$\begin{cases} \min F(u) := \dfrac{1}{2}\|Hu - u_d\|^2 + \lambda\Phi(u), \\ u \in \mathbb{R}^N,\ u \in \{0,1\} \end{cases}$$

Recall that

$$u \in \{0,1\} \iff u_i \in \{0,1\} \quad \forall i = 1, \cdots, N,$$

where $u = (u_i)_{1 \le i \le N}$.

The result of Theorem 2.1 allows us to assume that Φ is $\mathcal{C}^2$. Problem (4) obviously has a solution since F is continuous on a compact set. In the next propsoition, we give an equivalent formulation of (4):

Proposition 2.2. *Problem* (4) *is equivalent to*

$$\min\{F(u) \mid (u,v) \in \mathcal{D},\ (u,v)_N = 0\}$$

where

$$F(u) = \frac{1}{2}\|Hu - u_d\|^2 + \lambda\Phi(u), \tag{8}$$

and

$$\mathcal{D} = \{(u,v) \in \mathbb{R}^N \times \mathbb{R}^N \mid u + v = 1,\ u \ge 0,\ v \ge 0\}.$$

Proof. Assume $u \in \{0,1\}$ and set $v = 1 - u$, then $(u,v) \in \mathcal{D}$. In addition

$$\forall i \qquad u_i = 1 \iff v_i = 0 \quad \text{and} \quad u_i = 0 \iff v_i = 1,$$

so that $(u,w)_N = 0$.
Conversely, let $(u,v) \in \mathcal{D}$. Then, as $u,\ v \ge 0$ we get

$$(u,v)_N = 0 \Longrightarrow \forall i = 1, \cdots, N \quad u_i v_i = u_i(1 - u_i) = 0.$$

This implies that $u \in \{0,1\}$. Both feasible domains (and objective functions) are the same, thus the problems are equivalent. □

Note that $\mathcal{D}$ is a closed, convex subset of $[0,1]^N \times [0,1]^N$. In the sequel we consider the abstract problem

$$(\mathcal{P}) \qquad \min\{F(u) \mid (u,v) \in \mathcal{D},\ (u,v)_N = 0\}$$

where F is $\mathcal{C}^1$ and

$$\mathcal{D} = \{(u,v) \in \mathbb{R}^N \times \mathbb{R}^N \mid u + v = 1,\ u \ge 0,\ v \ge 0\}. \tag{9}$$

Remark 2.3. It is sufficient to assume that F is continuous to get existence and convergence results for approximating/penalizing processes (order 0). However, keeping in mind the first order optimality conditions, we state that F is of class $\mathcal{C}^1$.

3. An approximate formulation

3.1. A relaxed problem

In order to relax the complementarity constraint "$(u,v)_N = 0$" we introduce a $\mathcal{C}^1$ function $\theta_r : \mathbb{R}^+ \to [0,1[$, with $r > 0$ such that the following properties are satisfied ([8]):

$$\theta_r \text{ is nondecreasing, and } \theta_r(1) < 1, \tag{10a}$$

$$\forall r > 0 \quad \theta_r(0) = 0, \tag{10b}$$

$$\forall x > 0 \quad \lim_{r\to 0} \theta_r(x) = 1. \tag{10c}$$

Example 3.1. The functions below satisfy assumption (10) (see [8]):

$$\theta_r^1(x) = \frac{x}{x+r},$$

$$\theta_r^{W_k}(x) = 1 - e^{-(\frac{x}{r})^k},$$

$$\theta_r^{log}(x) = \frac{\log(1+x)}{\log(1+x+r)}.$$

Functions θ_r are built to approximate the complementarity constraint in the following sense:

$$\forall (x,y) \in \mathbb{R}\times\mathbb{R} \quad xy = 0 \iff \theta_r(x) + \theta_r(y) \simeq 1 \quad \text{for } r \text{ small enough.}$$

More precisely, we have the following proposition.

Proposition 3.2. *Let $(u,v) \in \mathcal{D}$ and θ_r satisfying (10). Then*

$$(u,v)_N = 0 \Longrightarrow \forall i = 1,\cdots,N \quad \theta_r(u_i) + \theta_r(v_i) = \theta_r(1) \le 1.$$

Proof. Let (u,v) be in $\mathcal{D}$. As $u_i v_i \ge 0$ for every i then

$$(u,v)_N = 0 \Longrightarrow \forall i = 1,\cdots,N \quad u_i v_i = 0.$$

Without loss of generality, let us assume that $u_i = 0$. Then $v_i = 1$ and

$$\theta_r(u_i) + \theta_r(v_i) = \theta_r(0) + \theta_r(1) = \theta_r(1).$$

□

The converse implication if not true of course but almost true. More precisely, let us define, for any $r > 0$

$$(\mathcal{P}_r) \quad \begin{cases} \min F(u) \\ (u,v) \in \mathcal{D}, \\ 0 \le \theta_r(u_i) + \theta_r(v_i) \le 1, \ \forall i = 1,\cdots,N \end{cases}$$

We claim that $(\mathcal{P}_r)$ is a good approximation of $(\mathcal{P})$ in the following sense:

Theorem 3.3. *Assume that θ_r satisfies assumptions (10). Then, for every $r > 0$, problem $(\mathcal{P}_r)$ has (at least) a solution $(u_r, v_r = 1 - u_r)$. Moreover*

$$\lim_{r\to 0} u_r = \bar{u},$$

where $\bar{u}$ is a solution to $(\mathcal{P})$.

In the sequel r and r_ε are nonnegative real numbers.

3.2. Proof of Theorem 3.3

The feasible domain of $(\mathcal{P}_r)$ is compact and the function F is continuous, so the existence of a solution is ensured.
The proof of convergence is not straightforward and we have to introduce another approximated problem $(\mathcal{P}^\varepsilon)$ such that $(\mathcal{P}_r)$ is *between* $(\mathcal{P})$ and $(\mathcal{P}^\varepsilon)$. To do this we approximate the complementarity constraint $xy = 0$ by $0 \le xy \le \varepsilon$ where $\varepsilon > 0$. We need the following lemma:

Lemma 3.4. *For every $\varepsilon > 0$ there exists $r_\varepsilon > 0$ such that*

$$\forall r \le r_\varepsilon,\ \forall x, y \in [0,1]\times[0,1]\ \ \theta_r(x) + \theta_r(y) \le 1 \Longrightarrow xy \le \varepsilon.$$

Proof. Let $\varepsilon > 0$ and assume that $\forall r > 0,\ \exists\, \tilde{r}$ such that $0 < \tilde{r} \le r$ and

$$\exists\, \tilde{x}_r, \tilde{y}_r \in [0,1]\times[0,1]\ \text{ such that } \theta_{\tilde{r}}(\tilde{x}_r) + \theta_{\tilde{r}}(\tilde{y}_r) \le 1 \text{ and } \tilde{x}_r\tilde{y}_r > \varepsilon.$$

Let us choose $r = \frac{1}{n}$ and denote $\tilde{r} = r_n \to 0,\ x_n := \tilde{x}_{r_n},\ y_n := \tilde{y}_{r_n}$ and $\theta_n := \theta_{r_n}$ so that

$$x_n y_n > \varepsilon,\ x_n \in [0,1],\ y_n \in [0,1] \text{ and } \theta_n(x_n) + \theta_n(y_n) \le 1.$$

As $(x_n)_{n\in\mathbb{N}}$ and $(y_n)_{n\in\mathbb{N}}$ are bounded one can extract subsequences still denoted similarly such that $x_n \to x$ and $y_n \to y$ with $x \in [0,1]$, $y \in [0,1]$ and $xy \ge \varepsilon$. Therefore x and y are nonzero and one can find $n_o \in \mathbb{N}$ such that

$$\forall n \ge n_o\ \ x_n > \rho > 0 \text{ and } y_n > \rho > 0,$$

where $\rho = \min\{\frac{\varepsilon}{2y}, \frac{\varepsilon}{2x}\}$. Here we use that θ_n is nondecreasing (10a). This yields that

$$\forall n \ge n_o\ \ \theta_n(x_n) + \theta_n(y_n) \ge 2\theta_n(\rho).$$

As $\theta_n(\rho) \to 1$ with (10c), this gives the contradiction. □

We can summarize as follows: $\forall \varepsilon > 0,\ \exists r_\varepsilon > 0,$ such that

$$\forall r \le r_\varepsilon,\ \forall (u,v) \in \mathcal{D}\ \ (u,v)_N = 0 \Longrightarrow \forall i\ \ \theta_r(u_i) + \theta_r(v_i) \le 1 \Longrightarrow (u,v)_N \le N\varepsilon. \quad (11)$$

Now we introduce another approximated problem $(\mathcal{P}^\varepsilon)$, for every $\varepsilon > 0$:

$$(\mathcal{P}^\varepsilon) \quad \begin{cases} \min F(u) \\ (u,v) \in \mathcal{D}, \\ 0 \le u_i v_i \le \varepsilon,\ \forall i = 1, \cdots, N \end{cases}$$

Once again $(\mathcal{P}^\varepsilon)$ obviously has at least one solution $(u^\varepsilon, v^\varepsilon)$. We first compare $(\mathcal{P}^\varepsilon)$ and $(\mathcal{P})$ with the next lemma.

Lemma 3.5. *Let ε tends to 0. Then u^ε (respectively v^ε) converges to $\bar{u}$ (resp. $1-\bar{u}$) (up to a subsequence) where $\bar{u}$ is a solution to $(\mathcal{P})$.*

Proof. For every $\varepsilon > 0$ the pair $(u^\varepsilon, v^\varepsilon)$ is bounded (since $\mathcal{D}$ is bounded) and one can extract a subsequence such that $(u^{\varepsilon_n}, v^{\varepsilon_n})$ converges to $(\tilde{u}, \tilde{v})$. As $0 \leq (u^{\varepsilon_n}, v^{\varepsilon_n})_N \leq N\varepsilon_n$ for every n it is clear that $(\tilde{u}, \tilde{v})_N = 0$ and that $(\tilde{u}, \tilde{v})$ is feasible for $(\mathcal{P})$. Therefore $\min(\mathcal{P}) \leq F(\tilde{u})$.
Let $\bar{u}$ be a solution to $(\mathcal{P})$. As $(\bar{u}, \bar{v} := 1 - \bar{u})$ is also feasible for $(\mathcal{P}^\varepsilon)$, for every ε we get

$$\forall \varepsilon \quad F(u^\varepsilon) \leq F(\bar{u}).$$

Passing to the limit gives $F(\tilde{u}) \leq F(\bar{u}) = \min(\mathcal{P})$. So $F(\tilde{u}) = \min(\mathcal{P})$ and $(\tilde{u}, \tilde{v})$ is a solution to $(\mathcal{P})$. □

Now we may end the proof of Theorem 3.3: let $\varepsilon > 0$ **be fixed** and $r \leq r_\varepsilon$ where r_ε is given by Lemma 3.4. So, any $(\mathcal{P}_r)$ feasible pair $(u, v := 1 - u)$ is feasible for $(\mathcal{P}^\varepsilon)$ as well. Therefore

$$\forall r \leq r_\varepsilon \quad F(u^\varepsilon) \leq F(u_r),$$

with the previous notations. As (u_r, v_r) is bounded one can extract a subsequence (denoted similarly) that converges to $(u^*, v^*) \in \mathcal{D}$. From Lemma 3.4 we get

$$\forall r \leq r_\varepsilon, \forall i = 1, \cdots, N \quad u_{r,i} v_{r,i} \leq \varepsilon.$$

The passage to the limit as $r \to 0$ gives

$$\forall i = 1, \cdots, N \quad u_i^* v_i^* \leq \varepsilon.$$

Let i be in $\{1, \cdots, N\}$ and assume $u_i^* \neq 0$. One can find $r^i > 0$ and $\rho_i > 0$ such that

$$\forall r \leq r^i \quad u_{r,i} > \rho_i > 0.$$

As a result of (10a) we get

$$\forall r \leq r^i \quad \theta_r(u_{r,i}) \geq \theta_r(\rho_i),$$

and with (10c)

$$\lim_{r \to 0} \theta_r(u_{r,i}) = 1.$$

Assume that $v_i^* \neq 0$: the same technique also gives $\lim_{r \to 0} \theta_r(v_{r,i}) = 1$. As $0 \leq \theta_r(u_{r,i}) + \theta_r(u_{r,i}) \leq 1$ this results in a contradiction. So we get either $u_i^* = 0$ or $v_i^* = 0$, that is $u_i^* v_i^* = 0$. Finally, we obtain $(u^*, v^*)_N = 0$.
So (u^*, v^*) is feasible for $(\mathcal{P})$. In addition, $F(u_r) \leq F(\bar{u})$ for every r where $\bar{u}$ is a solution to $(\mathcal{P})$. This yields that $F(u^*) \leq F(\bar{u})$. □

3.3. A relaxed optimality system

Now we consider problem $(\mathcal{P}_r)$ for $r > 0$ and derive optimality conditions. The problem can also be formulated as:

$$\min\{F(u) \mid G^r(u) \leq 0,\ u \in \mathbb{R}^N\}$$

where $G^r(v) = \begin{bmatrix} -u \\ u-1 \\ \Psi_r(u)-1 \end{bmatrix}$, and

$$\Psi_r(u) = \Theta_r(u) + \Theta_r(1-u) \quad \text{with } \Theta_r(u) = \begin{bmatrix} \theta_r(u_1) \\ \vdots \\ \theta_r(u_N) \end{bmatrix}. \tag{12}$$

Let us call $\bar{u}$ a solution to $(\mathcal{P}_r)$. We use the classical Mangasarian-Fromowitz (MF) qualification condition at $\bar{u}$ to get Lagrange multipliers. More precisely, following [7] p. 235, we are going to find $w \in \mathbb{R}^N$ such that

$$(\nabla G_k^r(\bar{u}), w)_N < 0 \quad \text{if } G_k^r(\bar{u}) = 0,\ k = 1, \cdots, N+2.$$

In our case the above condition reads:

$$\begin{gathered} w_i < 0 \quad \text{if } \bar{u}_i = 1 \\ w_i > 0 \quad \text{if } \bar{u}_i = 0 \\ [\theta_r'(\bar{u}_i) - \theta_r'(1-\bar{u}_i)]\, w_i < 0 \quad \text{if } \theta_r(\bar{u}_i) + \theta_r(1-\bar{u}_i) = 1. \end{gathered}$$

From this point on, we assume in addition that

$$\theta_r \text{ is strictly concave and } \mathcal{C}^2, \tag{13}$$

so that the function $\psi_r : [0,1] \to [\theta_r(1), 2]$, defined by $\psi_r(x) := \theta_r(x) + \theta_r(1-x)$ for every $x \in [0,1]$ is strictly concave and $\mathcal{C}^2$ as well. Note that functions of Example 3.1 are strictly concave and $\mathcal{C}^\infty$.

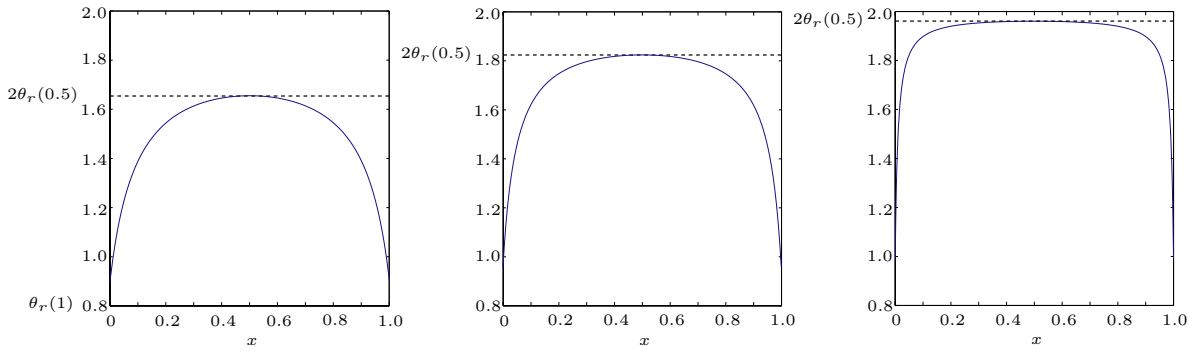

Figure 3.1: Function $\psi_r : x \mapsto \theta_r^1(x) + \theta_r^1(1-x)$ for different values of r and $\theta_r(x) = \frac{x}{x+r}$

Let i be in $\{1, \cdots, N\}$ and consider $\bar{u}_i \in [0,1]$;

- If $\bar{u}_i = 1$ then $\theta_r(\bar{u}_i) + \theta_r(1-\bar{u}_i) = \theta_r(1) < 1$ and we may choose $w_i = -1$ for example.
- Similarly, if $\bar{u}_i = 0$ one can choose $w_i = 1$.
- It remains the case where $0 < \bar{u}_i < 1$ and $\psi_r(v_i) = \theta_r(\bar{u}_i) + \theta_r(1-\bar{u}_i) = 1$.
  As $\psi_r : [0,1] \to [\theta_r(1), 2]$ is continuous, strictly concave, and symmetric with

respect to $v = \frac{1}{2}$, its maximum is attained at $x = \frac{1}{2}$.
Moreover we get for r small enough

$$\psi_r\left(\frac{1}{2}\right) = 2\theta_r\left(\frac{1}{2}\right) > 1 = \psi_r(\bar{u}_i) > \theta_r(1).$$

Therefore, with Rolle's Theorem we claim that $\psi_r'(\bar{u}_i) \neq 0$. So, there exists $w_i = -\psi_r'(\bar{u}_i)$ such that $\psi_r'(\bar{u}_i)w_i < 0$.

We conclude that Lagrange multipliers exist:

Theorem 3.6. *Assume that F is $\mathcal{C}^1$, that (10) and (13) hold, and let $(u_r, v_r = 1-u_r)$ be a solution to $(\mathcal{P}_r)$. Then, for r small enough, there exists $(\beta_r^1, \beta_r^2, \mu_r) \in \mathbb{R}^N \times \mathbb{R}^N \times \mathbb{R}^N$ such that:*

$$DF(u_r) + \beta_r^1 - \beta_r^2 + \mu_r \cdot D\Psi_r(u_r) = 0, \tag{14a}$$

$$\beta_r^1 \geq 0, \qquad \beta_r^2 \geq 0, \qquad \mu_r \geq 0, \tag{14b}$$

$$0 \leq u_r \leq 1, \qquad \Psi_r(u_r) = \Theta(u_r) + \Theta(1-u_r) \leq 1, \tag{14c}$$

$$(\beta_r^1, u_r)_N = (\beta_r^2, 1-u_r)_N = (\mu_r, \Psi_r(u_r) - 1)_N = 0. \tag{14d}$$

where

$$\mu_r \cdot D\Theta_r(u_r) := \begin{bmatrix} \mu_{r,1}\theta_r'(u_{r,1}) \\ \vdots \\ \mu_{r,N}\theta_r'(u_{r,N})] \end{bmatrix}.$$

Proof. It is straightforward since the (MF) qualification condition is satisfied at u_r (see [7]) □

4. A penalized formulation

In this section, we propose a penalization scheme to solve $(\mathcal{P})$. We consider the following sequence of penalized problems

$$(\widetilde{\mathcal{P}_r}) \quad \begin{cases} \min F(u) + \alpha(r) \displaystyle\sum_{i=1}^{N} [\theta_r(u_i) + \theta_r(1-u_i)] \\ u \in \mathbb{R}^N,\ 0 \leq u_i \leq 1,\ i = 1, \cdots, N \end{cases}$$

where $r > 0$ and α is a nonnegative real function satisfying

$$(H1) \qquad \lim_{r \to 0} \alpha(r) = +\infty$$

Remark 4.1. Any feasible point $(u, v := 1-u)$ for the initial problem $(\mathcal{P})$ satisfies

$$\sum_{i=1}^{N} [\theta_r(u_i) + \theta_r(1-u_i)] = N\theta_r(1) = \min_{(u,v)\in\mathcal{D}} \sum_{i=1}^{N} [\theta_r(u_i) + \theta_r(1-u_i)].$$

Lemma 4.2. *For every $r > 0$, problem $(\widetilde{\mathcal{P}_r})$ has at least one solution $(u_r, v_r := 1-u_r)$ and the corresponding value $F(u_r)$ is a lower bound for val$(\mathcal{P})$.*

Proof. The existence of an optimal solution is obvious since $\mathcal{D}$ is bounded and the objective function of $(\widetilde{\mathcal{P}_r})$ is continuous.
Moreover, the second property is a direct consequence of Remark 4.1. □

Theorem 4.3. *Assume that θ_r satisfies assumptions* (10) *and α satisfies* $(H1)$. *Thus any limit point of the sequence of optimal solutions of $(\widetilde{\mathcal{P}_r})$ is an optimal solution of* $(\mathcal{P})$.

Proof. For $r > 0$, let (u^r, v^r) denote an optimal solution to $(\widetilde{\mathcal{P}_r})$. The sequence $\{(u^r, v^r)\}$ is obviously bounded and we can extract a subsequence that converges to $(\tilde{u}, \tilde{v})$ in $\mathcal{D}$. Due to Lemma 4.2, we need to prove the feasibility (for $(\mathcal{P})$) of this limit point.
Let $(\bar{u}, \bar{v} := 1 - \bar{u})$ be a solution to $(\mathcal{P})$. As $(\bar{u}, \bar{v})$ is also feasible for $(\widetilde{\mathcal{P}_r})$, for every $r > 0$ we get for every $r \geq 0$

$$\begin{aligned} F(u^r) + \alpha(r) \sum_{i=1}^{N} [\theta_r(u_i^r) + \theta_r(v_i^r)] &\leq F(\bar{u}) + \alpha(r) \sum_{i=1}^{N} [\theta_r(\bar{u}_i) + \theta_r(\bar{v}_i)] \\ &\leq F(\bar{u}) + \alpha(r) N \theta_r(1). \end{aligned}$$

Since F takes only positive values and $\theta_r(u_i^r) + \theta_r(v_i^r) \geq \theta_r(1)$ for every i, we obtain

$$0 \leq \sum_{i=1}^{N} [\theta_r(u_i^r) + \theta_r(v_i^r)] - N\theta_r(1) \leq \frac{F(\bar{u})}{\alpha(r)}.$$

$$\forall i \quad \lim_{r \to 0} \theta_r(u_i^r) + \theta_r(v_i^r) = 1.$$

Suppose that $(\tilde{u}, \tilde{v})$ is not feasible for $(\mathcal{P})$ so that, for some $i \in \{1, ..., N\}$

$$\exists \delta > 0, \quad \text{such that } \min(\tilde{u}_i, \tilde{v}_i) > \delta.$$

We have

$$\exists r_0 > 0 \ \text{ such that } \forall r < r_0, \quad \min(u_i^r, v_i^r) > \frac{\delta}{2}$$

and, then for $r < r_0$

$$\theta_r(u_i^r) + \theta_r(v_i^r) > 2\theta_r(\frac{\delta}{2}).$$

Passing to the limit, we obtain the following contradiction

$$\lim_{r \to 0} \theta_r(u_i^r) + \theta_r(v_i^r) \geq 2$$

that completes the proof. □

4.1. An exact penalization property

Under an additional assumption on functions θ and α, we can prove some *exact penalization* property and avoid the problem of parameter tuning.
Indeed, all penalized problems $(\widetilde{\mathcal{P}_r})$ have the same feasible set, which is a simple bounded convex polytope. Thus, we need concavity property on the objective functions.
From now on, we suppose that functions θ are twice continuously differentiable and satisfy

$$(H2) \qquad \lim_{r\to 0} \alpha(r) \left(\max_{0\leq x\leq 1} \theta_r''(x) + \theta_r''(1-x) \right) = -\infty.$$

Remark 4.4. Assumption $(H2)$ is not very restrictive since it is satisfied (for example) by functions θ^1 and θ^{W_k} of Example 3.1, if α satisfies respectively $\alpha \geq \frac{1}{r}$ and $\alpha \geq \frac{1}{r^2}$.

Lemma 4.5. *Under $(H2)$ and for every $r > 0$ small enough the objective function of $(\widetilde{\mathcal{P}_r})$ is concave.*

Proof. Let r be sufficiently small. The first part of the objective function (F) is C^2 and the second one $(\alpha(r) \sum_{i=1}^N [\theta_r(u_i)+\theta_r(1-u_i)])$ is strongly concave with a sufficiently high modulus, thus the entire objective function is necessarily concave. □

Using a well known convex analysis result, we can establish the following lemma:

Lemma 4.6. *Under $(H2)$ and for every $r > 0$ small enough, all optimal solutions of $(\widetilde{\mathcal{P}_r})$ are extremal points of $\mathcal{D}$ (and then are feasible for $(\mathcal{P})$).*

Proof. Since the feasible domain $\mathcal{D}$ is a bounded convex polytope and the objective function is concave, this result is a direct application of [9] Corollary 32.3.3. □

Theorem 4.7. *Assume that θ_r and α meet assumptions (10), $(H1)$ and $(H2)$. Then for sufficiently small r, problems $(\widetilde{\mathcal{P}_r})$ and $(\mathcal{P})$ are equivalent and have the same optimal solutions.*

Proof. Let $r > 0$ be sufficiently small to apply Lemma 4.6 and let (u^r, v^r) be an optimal solution to $(\widetilde{\mathcal{P}_r})$. By using Lemma 4.6 and Lemma 4.2, we know that (u^r, v^r) is a feasible point for $(\mathcal{P})$ and that $F(u_r) \leq val(\mathcal{P})$. We can then conclude that $S(\widetilde{\mathcal{P}_r}) \subset S(\mathcal{P})$ and $F(u_r) = \inf(\mathcal{P})$. (Here, $S(\mathcal{P})$ denotes the set of solutions of $\mathcal{P}$.)
Conversely, let $(\bar{u}, \bar{v} := 1 - \bar{u})$ be an optimal solution to $(\mathcal{P})$. This point is obviously feasible for $(\widetilde{\mathcal{P}_r})$ and satisfies $F(\bar{u}) = \inf(\mathcal{P}) \leq F(u_r)$. Moreover, Remark 4.1 yields

$$\alpha(r) \sum_{i=1}^N [\theta_r(\bar{u}_i) + \theta_r(1-\bar{u}_i)] \leq \alpha(r) \sum_{i=1}^N [\theta_r(u_i^r) + \theta_r(1-u_i^r)].$$

So that $(\bar{u}, \bar{v}) \in S(\widetilde{\mathcal{P}_r})$. □

5. Numerical realization

5.1. Introduction

We have used the previous formalism to compute solutions to problem (4) (which fits the original model) with F defined by (8). Then we used the numerical implementation (that we detail thereafter) to give an equivalent formulation of (4) that allows us to deal with an objective function that is no longer $\mathcal{C}^1$. More precisely we have tested a cost functional defined by

$$F_p(u) = \frac{1}{2}\|Hu - u_d\|_N^2 + \lambda\Phi(u), \tag{15}$$

where $\lambda \geq 0$. The choice $\lambda = 0$ corresponds to a model that does not involve the total variation of u.
We have performed numerical experiments for both

$$(\mathcal{P}_r) \quad \begin{cases} \min F(u) \\ (u,v) \in \mathcal{D}, \\ 0 \leq \theta_r(u_i) + \theta_r(v_i) \leq 1, \ \forall i = 1, \cdots, N \end{cases}$$

and

$$(\widetilde{\mathcal{P}_r}) \quad \begin{cases} \min F(u) + \alpha(r) \displaystyle\sum_{i=1}^{N} [\theta_r(u_i) + \theta_r(1-u_i)] \\ u \in \mathbb{R}^N, \quad 0 \leq u_i \leq 1, \ i = 1, \cdots, N \end{cases}$$

where $r > 0$ and α is a nonnegative real function satisfying $\lim_{r \to 0} \alpha(r) = +\infty$.

We first computed solutions to $(\widetilde{\mathcal{P}_r})$ using classical methods described below. However, the problem we consider lies in a very specific physical context: we know that during the tomographic process, the global mass of the object is conserved. This means that, at least theoretically, the mass $\sum_i u_i$ remains constant. Because of the noise, this is not the case: so following [5] we add a *physical* constraint to problem $(\mathcal{P}_r)$, namely

$$m_\sigma \leq \sum_{i=1}^{N} u_i \leq M_\sigma, \tag{16}$$

where $m_\sigma = (1-2\sigma)\sum_{i=1}^{N} v_i$, $M_\sigma = (1+2\sigma)\sum_{i=1}^{N} v_i$, $v = H^{-1}u_d$ and σ is the gaussian noise standard deviation. Practically, this constraint speeds up the convergence and provides more accuracy.
As we have noticed that the computation of $(\widetilde{\mathcal{P}_r})$ solutions is more efficient, we shall report briefly on $(\mathcal{P}_r)$.

5.2. Discretization process

The discretized image is squared and represented by a $2M \times 2M$ array identified with a $4M^2$ vector. Due to the symmetry, it is sufficient to adress half an image (of size $M \times 2M$). In the sequel we set $N = 2M^2$, $X = \mathbb{R}^{M \times 2M}$ and $Y = X \times X$, endowed with

the usual scalar product $(u,v)_X = \sum_{i=1}^{M}\sum_{j=1}^{2M} u_{ij}v_{ij}$. The discretization step is $h=1$, as usual in discrete image processing. For $g=(g^1,g^2)\in Y$, denote

$$|g_{i,j}| = \sqrt{(g^1_{i,j})^2 + (g^2_{i,j})^2}.$$

The image is represented by the intensity function u. It is assumed to be piecewise constant. We denote by

$$u^j = u(i,j), \quad i=1,M,\ j=1,2M \quad \text{and} \quad u=(u^j)_{1\leq j\leq 2M}.$$

The Radon measure Du is approximated as follows. For $u\in X$, Du is identified with a vector of Y of coordinates $(Du)_{i,j} = ((Du)^1_{i,j},(Du)^2_{i,j})$ defined by

$$(Du)^1_{i,j} = \begin{cases} u_{i+1,j}-u_{i,j} & \text{if } i<M \\ 0 & \text{if } i=M \end{cases} \qquad (Du)^2_{i,j} = \begin{cases} u_{1,j+1}-u_{i,j} & \text{if } j<2M \\ 0 & \text{if } j=M. \end{cases}$$

The total variation is then approximated by $\Phi(u) = \sum_{i=1}^{M}\sum_{j=1}^{2M}|(Du)_{i,j}|$. Function Φ from X to $\mathbb{R}^+$ is convex, nonnegative and nondifferentiable.

In order to compute the discretized projection operator we apply the principle that that if $u\in L^\infty(\mathbb{R}_+\times\mathbb{R})$ with compact support in Ω, then

$$(\mathcal{H}_o u)(y,z) = 2\int_{|y|}^{+\infty} u(r,z)\,\frac{r}{\sqrt{r^2-y^2}}dr, \tag{17}$$

a.e. $y,z\in\mathbb{R}$. Furthermore, the matrix H_o of the discretized projection operator related to $\mathcal{H}_o$ is a $2M^2\times 2M^2$ matrix

$$H_o = \begin{pmatrix} A & 0 & \cdots & 0 \\ 0 & A & 0 & \cdots \\ \vdots & \ddots & A & \ddots \\ \cdots & \cdots & 0 & A \end{pmatrix} \quad \text{and} \quad U = \begin{pmatrix} U^1 \\ \vdots \\ U^{2M} \end{pmatrix}$$

where A stands for the projection matrix $M\times M$ with respect to a line $u^j := u(:,j)$. A direct computation with formula (17) gives: $A = ((a_{i,j})_{1\leq i,j\leq M})$ with

$$a_{i,j} = 2\begin{cases} 0 & \text{if } j<i \\ \sqrt{(j+1)^2-i^2}-\sqrt{j^2-i^2} & \text{if } i\leq j\leq M-1. \end{cases}$$

Tests have been performed with the synthetic object we described in Section 1. The original image has been perturbed with two additional perturbations due to the experimental setup as in [1, 2]:

- A *blur*, due to the detector response and the X-ray source spot size. To simplify, it is assumed that the effect $\mathcal{B}$ of the blur is linear, and can be written

$$\mathcal{B}v = \mathcal{K} * v \tag{18}$$

where $*$ is the usual convolution operation, v is the projected image, and $\mathcal{K}$ is a positive symmetric kernel with compact support and such that $\int \mathcal{K}d\mu = 1$.

- A *noise*, assumed to be an additive Gaussian white noise, denoted τ, of zero mean and of standard deviation σ.

Other perturbations, such as scattered field or motion blur, are not taken into account in our study. With these assumptions, the projection of an object u is

$$u_d = \mathcal{B}\mathcal{H}_o u + \tau.$$

A comparison between the theoretical projection $\mathcal{H}_o u$ and the perturbed one is provided on Fig. 1.2 (b) and (c). All numerical experiments have been done with MATLAB© software.

5.3. Numerical results

In all of our numerical experiments, we used the same function $\theta_r = \theta_r^{W_1}$ (this function was slightly more efficient than $\theta_r = \theta_r^1$) and fixed step-sizes for the gradient and mutiplier displacements. We used a stopping criterion depending on the relative variation of the cost functional

$$\left| \frac{F(u^{n+1}) - F(u^n)}{F(u^n)} \right| \leq \text{tol}$$

where tol was set to $1e-3$ with a maximal number of iterations $itmax = 500$. The image size is $M = 256$ so that $N = 2 * 256^2 = 131\,072$. As in [1, 2] the initial guess is $H^{-1}(u_d)$.

We first present some numerical results for the relaxation and penalization approaches where the binarity approximation parameter is fixed to $r = 1e-5$ (we shall justify this choice later).

Note that the lack of convexity does not allow to assert that a solution is a global minimum. Only local minima can be reached a priori. Furthermore, even if a solution happens to be a glocal minimum we cannot ensure uniqueness.

5.3.1. Relaxation approach

The following table and figure report our results for different values of the regularization parameter λ when adding the *mass conservation* constraint (16):

λ	# iterations	$F(u^n)$	$\frac{\|u^{n+1}-u^n\|_\infty}{\|u^n\|_\infty}$	$\frac{\|u^n-u\|_{fro}}{4N^2}$	CPU time (s)
0.1	325	0.0200	7.11e-03	8.892e-4	102.64
1	180	0.0475	3.92e-03	8.797e-4	55.62
2	185	0.0528	3.86e-03	6.254e-4	57.48
5	170	0.0656	4.17e-03	5.075e-4	52.76
10	155	0.1024	3.75e-03	4.683e-4	48.63
15	149	0.1412	3.90e-03	4.767e-4	46.35
20	321	0.1802	4.15e-03	4.782e-4	101.05

Table 5.1: Relaxation approach with the *mass conservation* constraint

Here $\frac{\|u^n-u\|_{fro}}{4N^2}$ is the normalized Frobenius norm of the difference of u^n and the original image u.

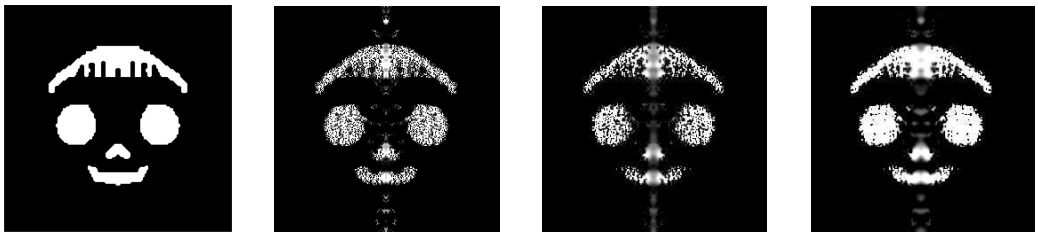

(a) The real object u. (b) $\lambda = 0.1$ (c) $\lambda = 1$ (d) $\lambda = 2$

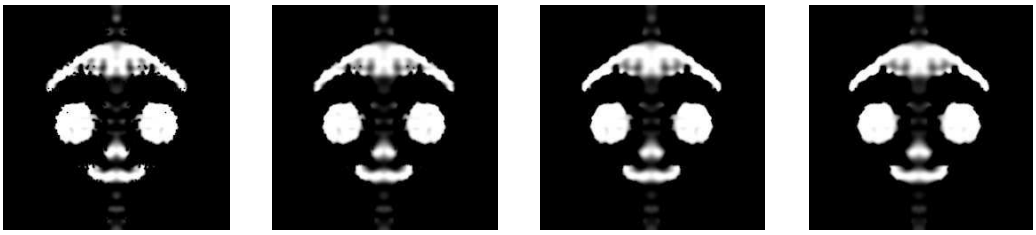

(e) $\lambda = 5$ (f) $\lambda = 10$ (g) $\lambda = 15$ (h) $\lambda = 20$

Figure 5.1: Relaxation approach with the *mass conservation* constraint for different values of λ

For the same parameters, we obtained the following results for the relaxed problem without the additional mass conservation constraint.

λ	# iterations	$F(u^n)$	$\frac{\|u^{n+1}-u^n\|_\infty}{\|u^n\|_\infty}$	$\frac{\|u^n-u\|_{fro}}{4N^2}$	CPU time (s)
0.1	325	0.0199	5.62e-03	8.760e-4	101.73
1	275	0.0485	3.64e-03	8.667e-4	86.70
2	185	0.0528	3.90e-03	6.236e-4	57.31
5	164	0.0654	3.86e-03	5.033e-4	53.66
10	152	0.1022	3.81e-03	4.693e-4	50.32
15	169	0.1408	3.93e-03	4.747e-4	53.33
20	324	0.1799	4.18e-03	4.786e-4	44.61

Table 5.2: Relaxation approach without the *mass conservation* constraint

We remark that the additional constraint when considering the relaxation approach does not significantly change the results and that $\lambda \in \{5, 10, 15\}$ seem to be good choices for the regularization parameter.

5.3.2. Penalization approach

For the penalized problem, the mass conservation constraint significantly improves the numerical results. We only present the numerical results in this case.

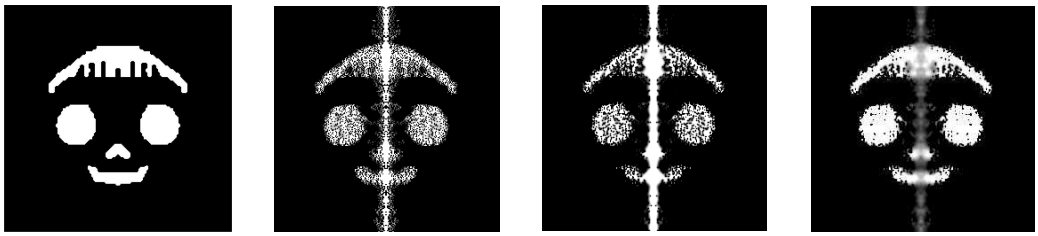

(a) The real object u. (b) $\lambda = 0.1$ (c) $\lambda = 1$ (d) $\lambda = 2$

(e) $\lambda = 5$ (f) $\lambda = 10$ (g) $\lambda = 15$ (h) $\lambda = 20$

Figure 5.2: Penalization approach with the mass conservation constraint for different values of λ

Once again $\lambda \in \{5, 10, 15\}$ seem to be good choices for the regularization parameter. The CPU times and the fourth column of Table 5.3 show that the iterates convergence is very fast, but the overall results as shown in the fifth column reveal that this technique performs less when compared to the relaxation approach results.

λ	# iterations	$F(u^n)$	$\frac{\|u^{n+1}-u^n\|_\infty}{\|u^n\|_\infty}$	$\frac{\|u^n-u\|_{fro}}{4N^2}$	CPU time (s)
0.1	140	0.0219	2.31e-5	1.039e-3	67.22
1	324	0.0496	1.74e-5	1.074e-3	157.02
2	54	0.0519	2.12e-5	6.220e-4	26.40
5	56	0.0647	2.64e-5	5.142e-4	26.98
10	90	0.1065	1.60e-5	5.518e-4	43.68
15	46	0.1557	5.58e-5	5.183e-4	21.50
20	325	0.4201	5.23e-4	1.187e-3	156.46

Table 5.3: Penalization approach with the mass conservation constraint

5.3.3. Results for differents binarity approximation parameters r

To measure the effect of the binarity approximation parameter, we did a number of numerical experiments when varying r. We consider the relaxation approach with the additional mass conservation constraint for a fixed value of the regularization parameter ($\lambda = 10$). The following table and figures present the results:

r	# iterations	$F(u^n)$	$\frac{\|u^{n+1}-u^n\|_\infty}{\|u^n\|_\infty}$	CPU time (s)
1.e-2	325	0.10962	2.64e-2	109.80
1.e-3	218	0.10341	5.874e-3	72.71
1.e-4	155	0.10252	3.72e-3	49.86
1.e-5	155	0.10245	3.75e-3	48.65
1.e-6	150	0.10238	3.90e-3	49.75

Table 5.4: Results for differents binarity approximation parameters

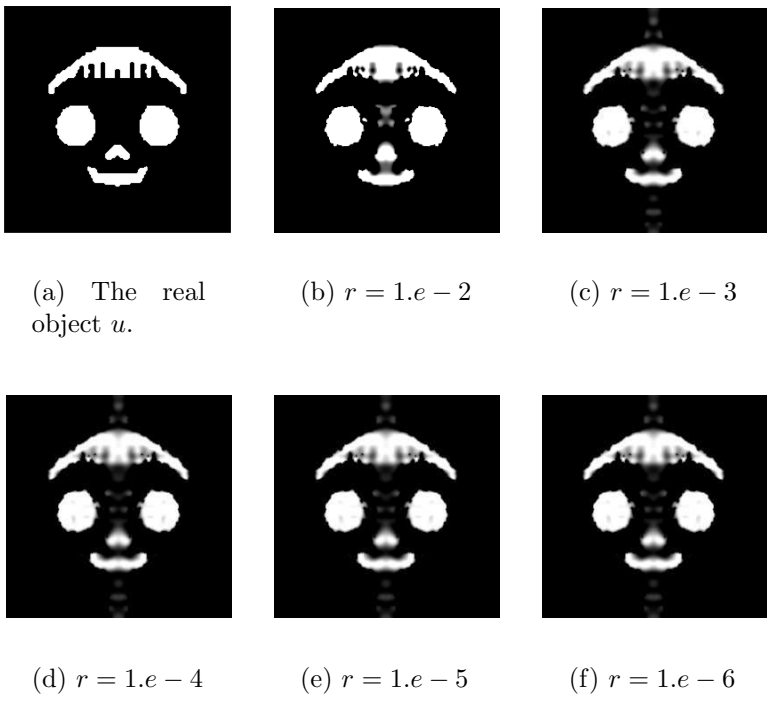

(a) The real object u. (b) $r = 1.e-2$ (c) $r = 1.e-3$

(d) $r = 1.e-4$ (e) $r = 1.e-5$ (f) $r = 1.e-6$

Figure 5.3: Relaxation approach with the mass conservation constraint for different values of r

These results prove that we do not need to perform a complicated strategy to move the binarity approximation parameter through 0. Fixing r small enough is sufficient to obtain ecellent results.

5.3.4. Cost behaviour and iterates evolution

For fixed values of the regularization parameter $\lambda = 10$ and the binarity approximation parameter $r = 1e-5$, the two following figures present the behaviour of the cost and iterates.

These figures correspond to the first approach (relaxation with mass constraints) but we observe almost the same results when applying the other approaches. It should be noted that our methods are not descent methods and that the significant improvements are made in the first iterations. Indeed, a simple rounding after a few iterates (65) gives the following result:

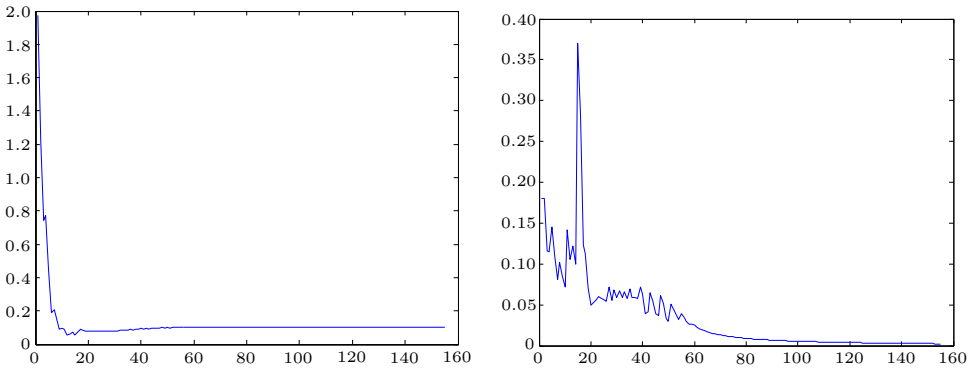

(a) cost evolution.

(b) evolution of $\frac{\|u^{n+1}-u^n\|_\infty}{\|u^n\|_\infty}$

Figure 5.4: Relaxation approach with the mass conservation constraint when $r = 1e-5$ and $\lambda = 10$

(a) The real object u.

(b) Solution after 65 iterations

(c) Round solution after 65 iterations $round(u_{65})$.

Figure 5.5: Round solution after 65 iterations when $r = 1e-5$ and $\alpha = 10$

References

[1] I. Abraham, R. Abraham, M. Bergounioux: An active curve approach for tomographic reconstruction of binary radially symmetric objects, in: Numerical Mathematics and Advanced Applications (Graz, 2007), K. Kunisch, G. Of, O. Steinbach (eds.), Springer, Berlin (2008) 663–670.

[2] R. Abraham, M. Bergounioux, E. Trélat: A penalization approach for tomographic reconstruction of binary axially symmetric objects, Appl. Math. Optim. 58 (2008) 345–371.

[3] L. Ambrosio, N. Fusco, D. Pallara: Functions of Bounded Variation and Free Discontinuity Problems, Oxford Mathematical Monographs, Oxford University Press, Oxford (2000).

[4] G. Aubert, P. Kornprobst: Mathematical Problems in Image Processing, Applied Mathematical Sciences 147, Springer, New York (2006).

[5] T. D. Capricelli, P. L. Combettes: A convex programming algorithm for noisy discrete

tomography, in: Advances in Discrete Tomography and its Applications, G. T. Herman, A. Kuba (eds.), Birkhäuser, Boston (2007) 207–226.

[6] A. Chambolle: An algorithm for total variation minimization and applications, J. Math. Imaging Vis. 20 (2004) 89–97.

[7] F. H. Clarke: Optimization and Nonsmooth Analysis, Classics in Applied Mathematics 5, SIAM, Philadelphia (1990).

[8] M. Haddou: A new class of smoothing methods for mathematical programs with equilibrium constraints, Pac. J. Optim. 5 (2009) 87–95.

[9] R. T. Rockafellar: Convex Analysis, Princeton University Press, Princeton (1996).

[10] J. A. Sethian: Theory, algorithms and applications of level set methods for propagating interfaces, in: Acta Numerica Vol. 5, A. Iserles (ed.), Cambridge University Press, Cambridge (1996) 309–395.